

## Supplementary Materials for **Microbial synthesis of highly dispersed PdAu alloy for enhanced electrocatalysis**

Jiawei Liu, Yue Zheng, Zilan Hong, Kai Cai, Feng Zhao, Heyou Han

Published 30 September 2016, *Sci. Adv.* **2**, e1600858 (2016)

DOI: 10.1126/sciadv.1600858

### **This PDF file includes:**

- fig. S1. The mechanism of biosynthesis.
- fig. S2. Morphological feature of different biocatalysts.
- fig. S3. Atomic ratio of as-prepared catalyst.
- fig. S4. Feature of graphene.
- fig. S5. CO stripping for the DPARH and commercial Pd/C.
- fig. S6. Ethanol electrooxidation activities of the DPARH synthesized under different conditions.
- fig. S7. Formic acid electrooxidation activities of the DPARH synthesized under different conditions.
- table S1. Electrocatalytic mass activities of different catalysts in previous studies.
- table S2. Atomic ratio of the DPARH from the XPS data.
- table S3. Electrocatalytic mass activities of DPARH synthesized under different conditions.
- References (55–64)

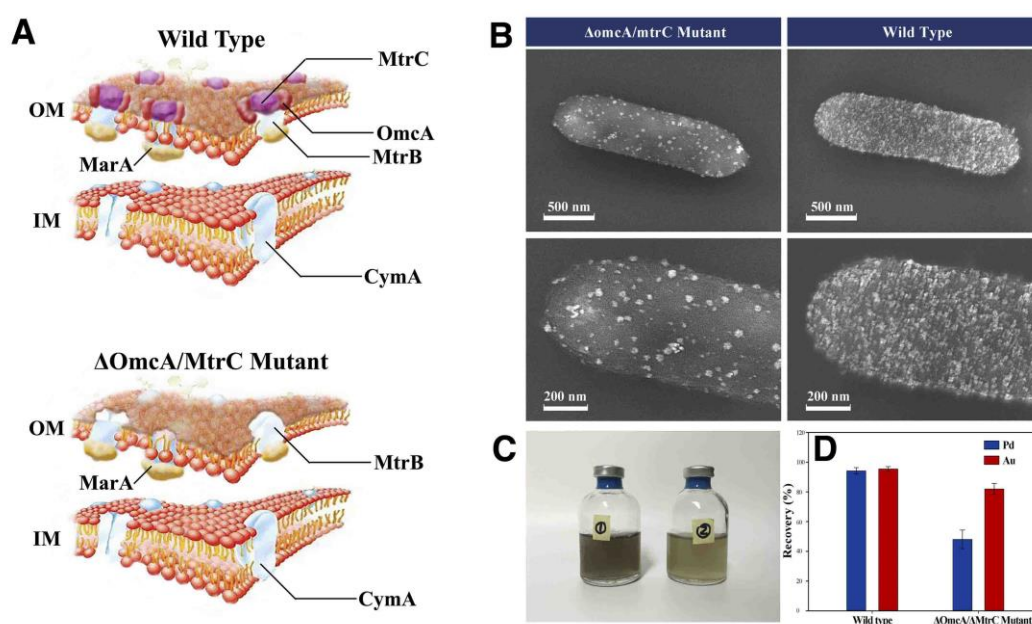


**fig. S1. The mechanism of biosynthesis.** (A) The function genes of extracellular electron transfer of wild type and  $\Delta$ omcA/mtrC mutant of *Shewanella oneidensis* MR-1, (B) The SEM images of wild type and  $\Delta$ omcA/mtrC mutant cells with Pd-Au nanoparticles, (C) The photo of wild type (left) and  $\Delta$ omcA/mtrC mutant (right) after Pd-Au reduction, (D) The recovery rate of Pd and Au after biosynthesis of Pd-Au nanoparticles between wild type and  $\Delta$ omcA/mtrC mutant cells.

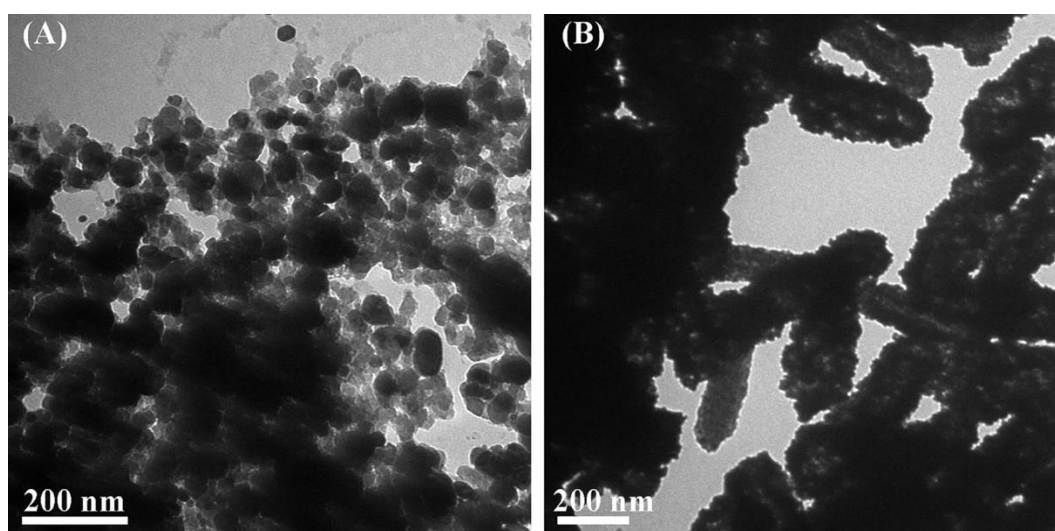


**fig. S2. Morphological feature of different biocatalysts.** (A) TEM image of 3D core/shell/shell bacteria/PdAu/GO hybrid biofilm (BPAGB) mixed with KOH at a mass ratio of 1:1, and carbonized in a tube furnace at 420°C (temperature ramp: 3°C/min) for 3h under argon flow. (B) TEM image of heteroatom doping bio-PdAu (DPA).

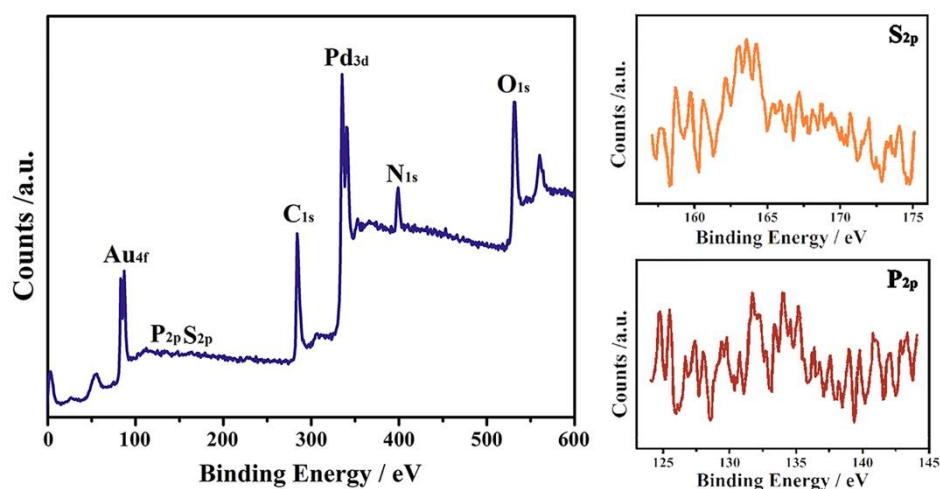


**fig. S3. Atomic ratio of as-prepared catalyst.** X-ray photoelectron spectroscopy of 3D porous heteroatom doping bio-PdAu/rGO hybrid (DPARH).

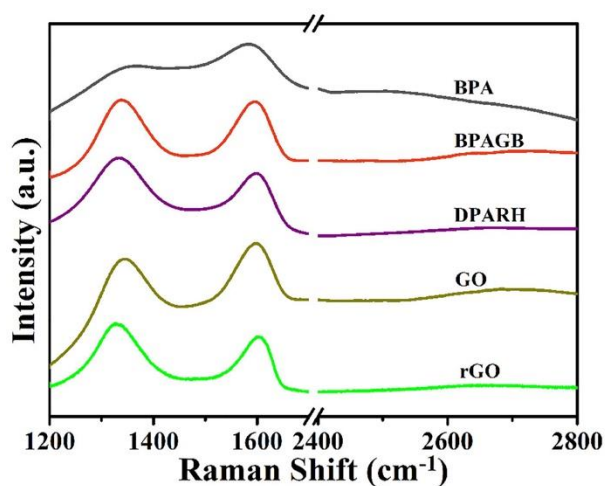


**fig. S4. Feature of graphene.** The Raman spectrum of core/shell bacteria/PdAu (BPA), 3D core/shell/shell bacteria/PdAu/GO hybrid biofilm (BPAGB), 3D porous heteroatom doping bio-PdAu/rGO hybrid (DPARH), GO, and rGO.

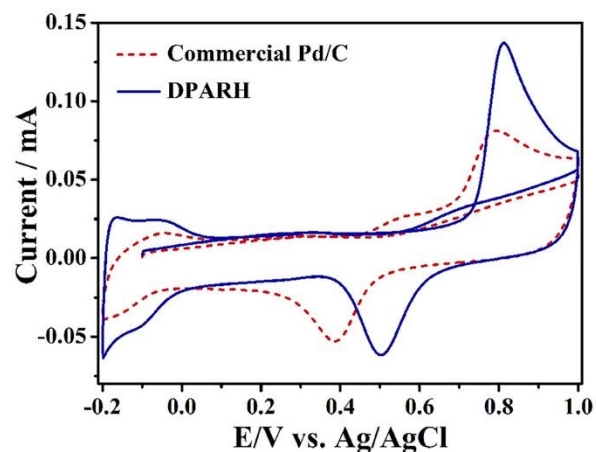


**fig. S5. CO stripping for the DPARH and commercial Pd/C.** They were performed in 0.1 M HClO<sub>4</sub> at a scan rate of 50 mV s<sup>-1</sup> from -0.2 V to 1.0 V vs. Ag/AgCl (saturated KCl). The solution was first purged with CO gas for 30 min and the electrode potential was kept at -0.1 V simultaneously in order to absorb CO on the surface of catalysts. Then, N<sub>2</sub> gas was bubbled into the solution for another 30 min under the same potential to remove the dissociative CO in the electrolyte before recording the CO stripping results.

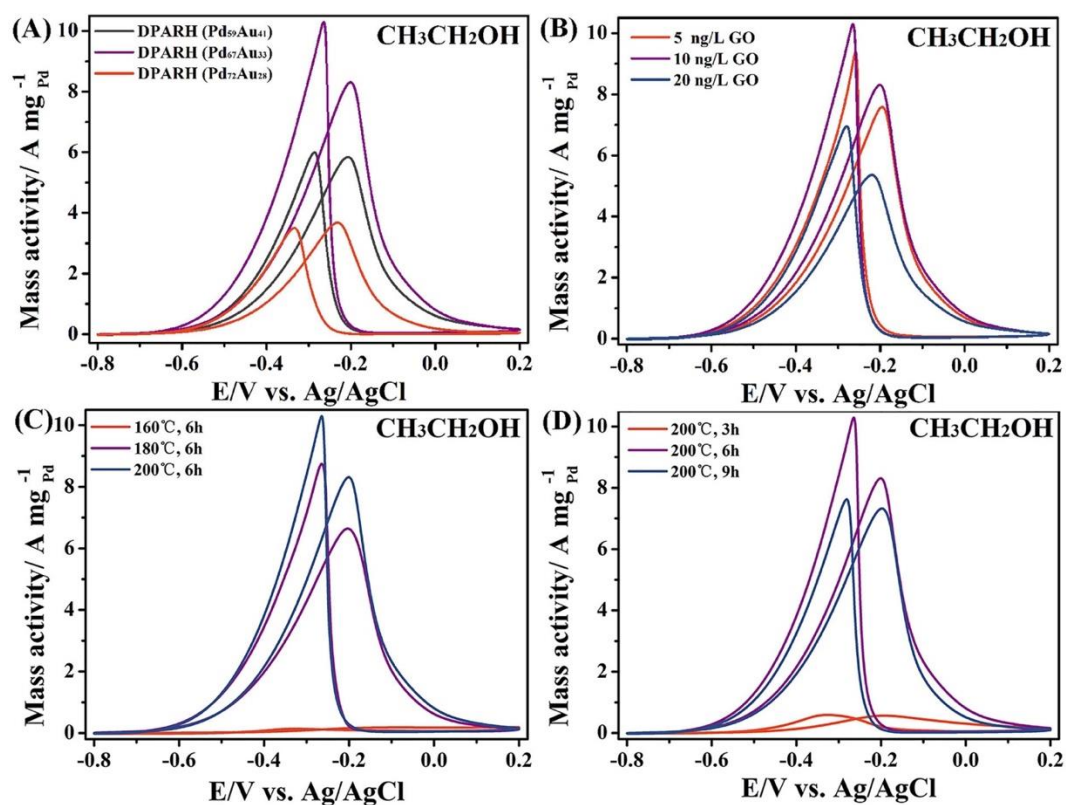


**fig. S6. Ethanol electrooxidation activities of the DPARH synthesized under different conditions. (A) Pd/Au ratio, (B) the amount of GO, (C) temperature, and (D) time of hydrothermal reaction. They were performed in 1 M KOH + 1 M ethanol at a scan rate of  $50 \text{ mV s}^{-1}$  vs. Ag/AgCl (saturated KCl).**

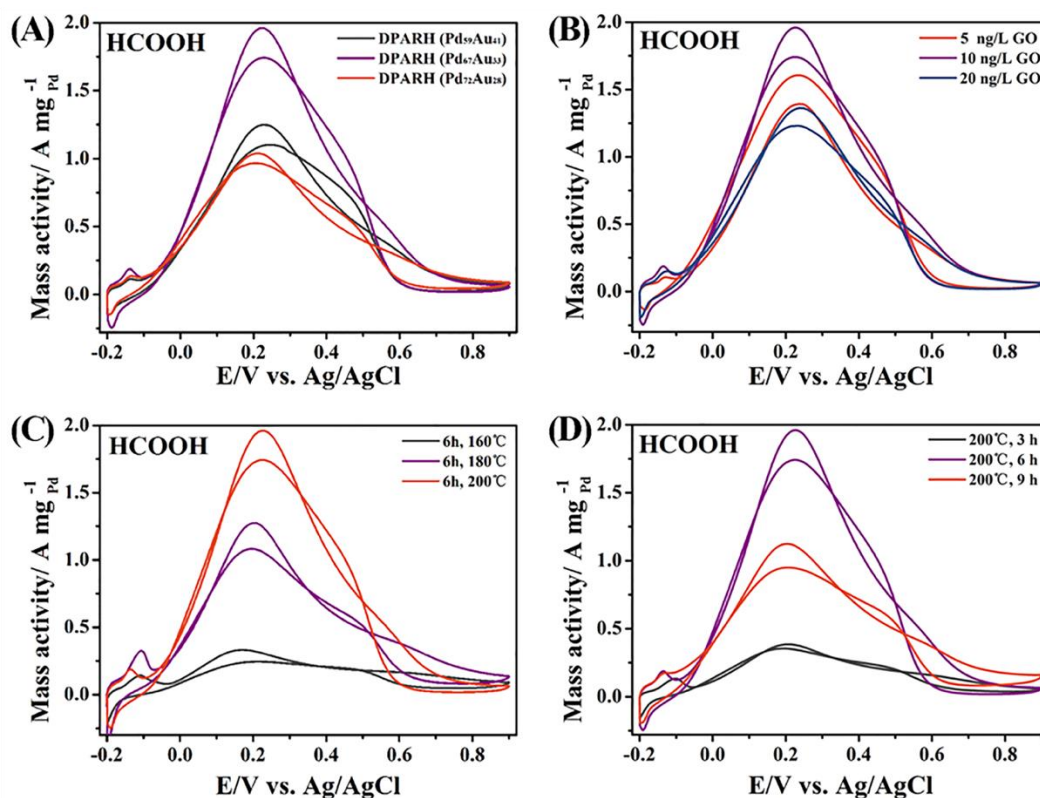


**fig. S7. Formic acid electrooxidation activities of the DPARH synthesized under different conditions. (A) Pd/Au ratio, (B) the amount of GO, (C) temperature, and (D) time of hydrothermal reaction. They were performed in 0.5 M H<sub>2</sub>SO<sub>4</sub> + 0.5 M HCOOH at a scan rate of 50 mV s<sup>-1</sup> vs. Ag/AgCl (saturated KCl).**

**table S1. Electrocatalytic mass activities of different catalysts in previous studies.**

0.5 M HCOOH+0.5M H <sub>2</sub> SO <sub>4</sub>			1M CH <sub>3</sub> CH <sub>2</sub> OH+1M KOH		
Catalyst	Mass activity	Reference	Catalyst	Mass activity	Reference
Pd–Ni <sub>2</sub> P/C	1.42 A mg <sup>-1</sup>	(13)	Pd <sub>80</sub> Cu <sub>20</sub> NNW	6.16 A mg <sup>-1</sup>	(12)
PdNiCu/C	0.792 A mg <sup>-1</sup>	(55)	Pd <sub>50</sub> Ag <sub>50</sub> BANWs	1.97 A mg <sup>-1</sup>	(56)
Pd/C-S	1.62 A mg <sup>-1</sup>	(57)	Pd/C	6.37 A mg <sup>-1</sup>	(58)
Pd arrow- headed tripods	0.493 A mg <sup>-1</sup>	(59)	Pd <sub>83</sub> Ni <sub>17</sub> Aerogel	3.6 A mg <sup>-1</sup>	(60)
PtAgCu@PtCu CSCNOs	0.31 A mg <sup>-1</sup>	(61)	ISCC- Au@AuPd NPs	4.15 A mg <sup>-1</sup>	(62)
Pd <sub>1</sub> Ni <sub>1</sub> -NNs /RGO	0.604 A mg <sup>-1</sup>	(63)	FePd–Fe <sub>2</sub> O <sub>3</sub> ( 3:5)/MWNTs	1.19 A mg <sup>-1</sup>	(64)
This work	2.044 A mg <sup>-1</sup>		This work	8.30 A mg <sup>-1</sup>	

**table S2. Atomic ratio of the DPARH from the XPS data.**

Name	Peak Binding Energy (eV)	I	S	At. %
Au4f	83.82	66740.36	6.250	2.51
S2p	163.5	3606.83	0.668	1.27
P2p	131.78	2066.23	0.486	1.00
C1s	284.55	60208.56	0.278	50.92
Pd3d	335.47	170442.62	5.356	7.48
N1s	399.15	22140.82	0.477	10.91
O1s	531.57	85952.8	0.780	25.91

**table S3. Electrocatalytic mass activities of DPARH synthesized under different conditions.**

Reaction conditions	Pd/Au ratio			Temperature (°C)			Time (h)			GO (ng/L)		
	59:41	67:33	72:28	160	180	200	3	6	9	5	10	20
Small molecule												
CH <sub>3</sub> CH <sub>2</sub> OH (A mg <sup>-1</sup> Pd)	5.84	8.31	3.68	0.18	6.63	8.31	0.56	8.31	7.32	7.59	8.31	5.36
HCOOH (A mg <sup>-1</sup> Pd)	1.24	1.96	1.04	0.33	1.27	1.96	0.38	1.96	1.12	1.61	1.96	1.36